Over 40-W Electric Power and Optical Data Transmission Using an Optical Fiber

Motoharu Matsuura, *Senior Member, IEEE*, Hayato Nomoto, Hikaru Mamiya, Tadanobu Higuchi, Denis Masson, and Simon Fafard

***Abstract*—Simultaneous over 40-W electric power and optical data transmission using an optical fiber is demonstrated for optically powered remote antenna units in future mobile communication networks. In this article, to further increase the delivered electric power by power-over-fiber link using a double-clad fiber, we improve the link design to extract a higher feed light power from the double-clad fiber output. Furthermore, to increase the electric power for driving remote antenna units, we employ a specially customized photovoltaic power converter that directly converts optical power into electric power. The photovoltaic power converter can input a feed light with power of over 20 W and has a high optical-to-electrical conversion efficiency of over 50%. As a result, the combination of the improved power-over-fiber link design and the use of the photovoltaic power converter successfully achieves the electric power delivery of up to 43.7 W. This is the highest electric power delivery demonstration by power-over-fiber with optical data signals using a single optical fiber, to the best of the authors' knowledge.**

***Index Terms*—Double-clad fiber (DCF), mobile communications, optical power delivery, photovoltaic power converter (PPC), power-over-fiber (PWoF), radio-over-fiber (RoF), remote antenna unit (RAU).**

I. Introduction

POWER-OVER-FIBER (PWoF) is an attractive approach for delivering electric power using optical fibers. As power lines, optical fibers are superior to conventional copper wires. For example, optical fibers are lightweight lines that are superior in corrosion resistance and robust to electromagnetic interference (EMI) and electric sparks [1], [2]. Several studies on various PWoF applications, such as sensors [3], [4], electrical current monitors [5], video cameras [6], and high-voltage gate drivers for semiconductor devices [7], have been conducted.

Manuscript received June 2, 2020; revised August 27, 2020; accepted September 16, 2020. Date of publication September 29, 2020; date of current version November 20, 2020. This work was supported in part by the Grant-in-Aid Scientific Research from the Ministry of Education, Culture, Sports, Science, and Technology (17H03260), and in part by the Telecommunication Advancement Foundation in Japan. Recommended for publication by Associate Editor J. Wang. *(Corresponding author: Motoharu Matsuura.)*

Motoharu Matsuura, Hayato Nomoto, Hikaru Mamiya, and Tadanobu Higuchi are with the Graduate School of Informatics, and Engineering, University of Electro-Communications, Chofu 182-8585, Japan (e-mail: m.matsuura@uec.ac.jp; h.nomoto@uec.ac.jp; h.mamiya@uec.ac.jp; t.higuchi@uec.ac.jp).

Denis Masson and Simon Fafard are with Broadcom, IFPD Division, Ottawa, ON K1A 0R6, Canada (e-mail: denis.masson@broadcom.com; simon.fafard@broadcom.com).

Color versions of one or more of the figures in this article are available online at https://ieeexplore.ieee.org.

Digital Object Identifier 10.1109/TPEL.2020.3027551

In future mobile communications, radio-over-fiber (RoF) will be an indispensable technology for transmitting radio-frequency (RF) data signals into optical fiber links between a central office (CO) and many remote antenna units (RAUs) [8], [9]. Indeed, it offers the benefits of broadband, low loss, immunity to EMI, and secure data transmission for RF data signals in the fiber links. A schematic view of the RoF-based mobile communication networks is shown in Fig. 1. In general, the electric power for driving RAUs is supplied by nearby power lines. However, if a power failure occurs owing to a natural disaster or electrical equipment failure, the mobile services will also stop. In addition, when installing an RAU, it is necessary to install electrical equipment and wiring from nearby power lines in addition to installing communication equipment. Therefore, it is important to provide simple and cost-effective mobile communication networks in the future.

To simultaneously transmit data and power into a single line, PWoF is a practical method. In RoF-based mobile communication networks, the power for driving each RAU can be sourced from a CO via each optical fiber link without installing electrical equipment and wiring, as shown in Fig. 1. Because PWoF is effectively used not only to transmit the power and the data, but also to centralize the power source in the CO, its usage makes it easier to manage the power supply system for an entire network. The power required for each RAU is determined by the amount of the mobile data traffic load, and the total power accounts for the majority of the power consumption of the entire network [10]. However, in current networks, the power for RAUs is always kept fully supplied on the assumption that each RAU supports not the "actual" traffic load but the "maximum" one. To solve this problem, a few research groups have shown that "sleep mode" power control of RAUs offers up to 60% energy saving in the networks [11], [12]. On the other hands, the power control by PWoF is more effective to reduce the total power supplied to RAUs over the entire day, because it is easy for the CO, which always knows the traffic load of each RAU, to precisely control the power supplied to each RAU in response to the temporary traffic load.

To drive a small to midsized RAU, more than 10-W of electric power is generally required. However, the electric power delivered by PWoF scheme is limited owing to the power density in the core area of the optical fibers. For example, in single-mode fibers (SMFs), which are most commonly used in optical fiber communications, the core area through which optical data and power propagate is extremely small, and not suitable for

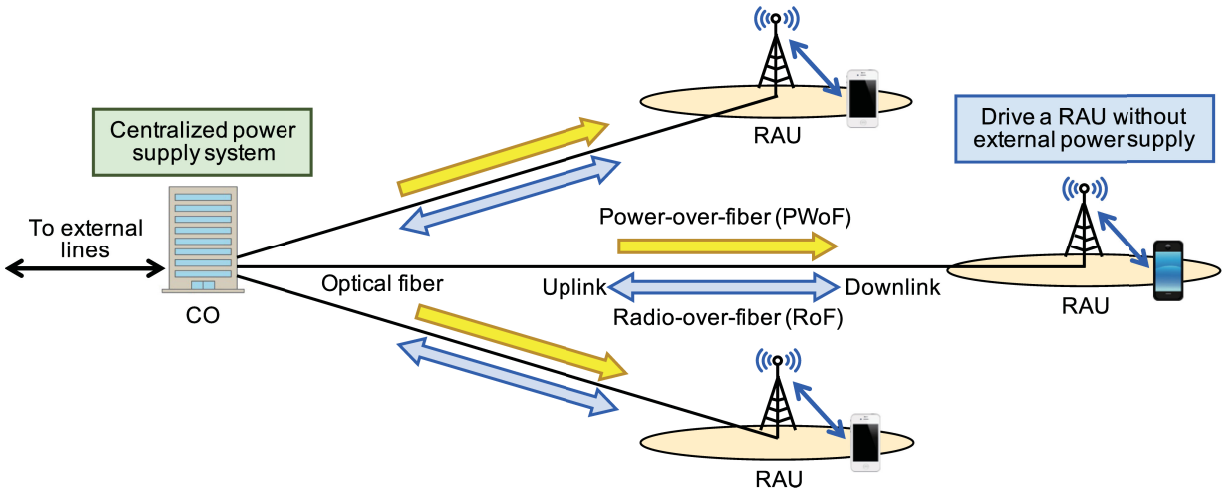

Fig. 1. Schematic view of RoF-based mobile communication networks with optically powered RAUs by PWoF using optical fibers.

such a high electric power delivery. Although multimode fibers (MMFs) have a larger core area than SMFs and are useful for higher power transmission, the data transmission speed is limited by the large core area, which gives rise to modal dispersion, and the crosstalk between the data and feed light for high-power transmission occurs in the same core [13]. Therefore, a more practical means is to use separate optical fibers for data transmission and power transmission [14], [15]. Optical cable can bundle multiple optical fibers. However, the number of optical fibers that can be installed in an optical cable is strictly limited in optical access networks [16]. It is, therefore, important to provide a PWoF technique that can transmit data and power over a single optical fiber. Indeed, over 6-W electric power delivery with optical data transmission by PWoF using a single MMF has been recently reported [17]. Such an approach promises to be practical and easy to mass production. Other approach have great potential and are being studied to obtain higher power feeding, for example, using photonic crystal fibers [18]−[20].

Double-clad fibers (DCFs) consist of a small single-mode (SM) core and a large inner cladding that surrounds the SM core. We previously proposed a PWoF scheme using DCFs and reported the experimental results [21]−[28]. The advantage of DCFs is that optical data signals can be transmitted into the SM core, whereas a high-power feed light can be transmitted into the inner cladding with a large core effective area that is over 240 times larger than that of the SM core. Therefore, it is useful for simultaneously transmitting optical data signals and high-power feed light into a single DCF. We previously demonstrated 60-W PWoF feed and bidirectional data transmission with good transmission performances [23], and an optically powered beam steering system over a 300-m DCF [24]. In addition, we achieved multichannel analog and digital data signals transmission and electrical power delivery of up to 7 W over a 300-m DCF [25]. Furthermore, we presented the temperature characteristics and transmission performance under a 150-W PWoF feed over a 1-km DCF [28]. However, because the transmission efficiency of the electric power in these studies was low, and the delivered electric power did not reach 10 W, which is necessary to drive a small to mid-sized RAU, it is essential to further improve the power transmission efficiency.

In this article, we present simultaneous transmission of over 40-W electric power and bidirectional data signals by PWoF using a single DCF. To increase the power transmission efficiency of a PWoF link, unlike in our previous studies, we improve the design of the PWoF link to transmit higher feed light power into the PWoF link. Furthermore, to increase the delivered electric power, we introduce a specially customized photovoltaic power converter (PPC), which converts optical power into electric power with a high optical-to-electrical (O/E) conversion efficiency [29], [30]. The PPC input has a feed light power of over 20 W and has an O/E conversion efficiency of over 50%. To the best of the authors' knowledge, this is the highest electric power delivery demonstration by PWoF with optical data signals using a single optical fiber.

The remainder of this article is organized as follows. In Section II, we describe the experimental setup for over 40-W electric delivery and bidirectional data transmission using a PWoF scheme. In Section III, we describe the two approaches used to improve the electric power delivery efficiency of the PWoF scheme. In Section IV, experimental evaluations of the electric power delivery efficiency and the bidirectional transmission performance of the data signals are described. In Section V, we discuss the feasibility and future perspective of the presented PWoF scheme. Finally, Section VI concludes this article.

II. Experimental Setup

Fig. 2 shows the experimental setup for the PWoF scheme using a 300-m DCF. In this setup, the downlink indicates data signal transmission from a CO to an RAU, while the uplink indicates data signal transmission from the RAU to the CO. Data signals were transmitted bidirectionally, and the feed light for powering the RAU was transmitted from the CO to the RAU. In the downlink transmitter, an electrical data signal was generated by a signal generator (SG) (MS2830 A, Anritsu Corp.). The data signal exhibited 64-quadrature amplitude modulation,

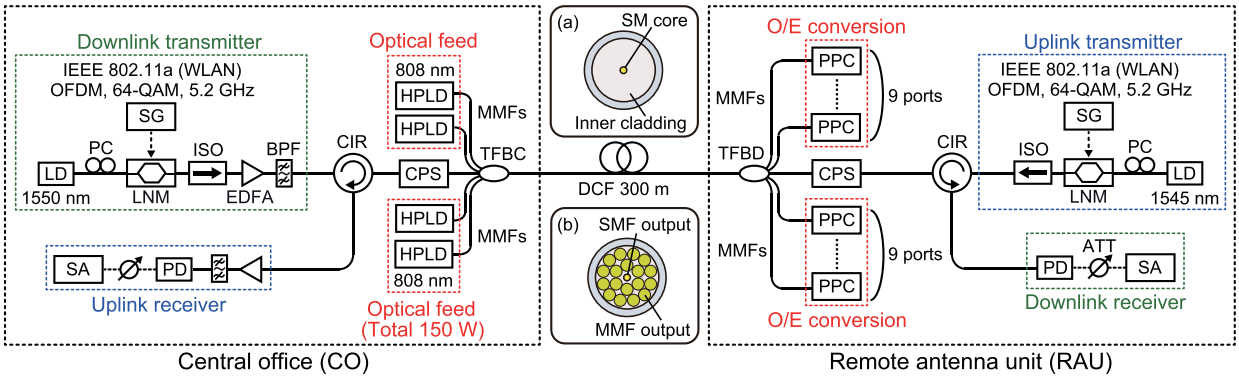

Fig. 2. Experimental setup for PWoF scheme using a 300-m DCF. PC: polarization controller, ISO: isolator, CIR: circulator, PD: photodiode, ATT: electrical attenuator, SA: signal analyzer. Insets show cross sections of (a) 300-m DCF and (b) TFBD.

orthogonal frequency division multiplexing at a carrier frequency of 5.2 GHz in accordance with IEEE 802.11a wireless local area network standard. An optical data signal was generated by the direct modulation using a laser-diode (LD) with a wavelength of 1550 nm, and the following $LiNbO_3$ modulator (LNM) with the electrical data signal. A polarization controller at the output of the LD was used to adjust the state of polarization of the LD output to obtain the highest quality of modulated signal. After passing through an isolator, the data signal was amplified by an erbium-doped fiber amplifier (EDFA), and passed through a bandpass filter (BPF) with a bandwidth of 3 nm to remove amplified spontaneous noise from the EDFA. Two circulators (CIRs) in the CO and RAU were used to pass through only the unidirectional data signals for bidirectional downlink and uplink data transmissions, respectively. After passing through a cladding power stripper (CPS), the data signal and the feed light generated by four high-power laser-diodes (HPLDs) with a wavelength of 808 nm were combined by a tapered fiber bundle combiner (TFBC). The CPS in the CO consisted of one SMF input port and one DCF output port, whereas the CPS in the RAU consisted of one DCF input port and one SMF output port. The role of the CPSs was to remove reflected and residual feed light components in the inner cladding of the DCF. The TFBC consisted of one DCF input port, four MMF input ports, and one DCF output port. The core diameter of the MMFs was 105 μm. Each core was tapered and directly connected to the inner cladding of the 300-m DCF. The total maximum power output from the four HPLDs was 150 W. The DCF was a commercially available optical fiber, and the diameters of the SM core, the inner cladding, and the outer cladding were 8 μm, 125 μm, and 180 μm, respectively, as shown in Fig. 2(a). The DCF was coated with a thin polymer, and the outer diameter was 250 μm, which was the same as that of conventional bare optical fibers. After the 300-m DCF transmission, the data signal and feed light were extracted by a tapered fiber bundle divider (TFBD), which consisted of one DCF input port, one DCF output port, and 18 MMF output ports. As shown in Fig. 2(b), the transmitted feed light component in the inner cladding of the TFBD was extracted from the 18 MMF output ports. Although we had used a TFBD with two or six MMF output ports in our previous studies [21], [28], by increasing the number of MMF output ports in this article, we attempted to increase the power of the feed light that can be extracted, and to improve the power transmission efficiency of the PWoF link. The detailed results are presented in Section III-A. The feed light at the output of each MMF was injected into a PPC, which was a specially customized device produced by Broadcom Inc. [29], [30]. The PPC had a higher capability of available optical injection power with a high O/E conversion efficiency. The detail characteristics are shown in Section III-B. In this experiment, there was only one the PPC. Therefore, to measure the delivered electric power at each MMF output port, the PPC was connected to each port in turn, and each converted electric power was measured. It should be noted that no output power fluctuation at each MMF output port was observed during the measurement. The data signal passed through a CPS and CIR, and was injected into a photodiode to convert the optical data signal into the electrical data signal. The output power of the electrical data signal was adjusted by an attenuator, and the signal was injected into a signal analyzer to measure the data transmission performance in terms of the error-vector magnitude (EVM). In the uplink transmission, an optical data signal at a wavelength of 1545 nm was generated in the uplink transmitter, and simultaneously transmitted with the downlink data signal to the same SM core in the PWoF link in the reverse direction. After passing through the CIR, CPS, and TFBD in the RAU, the uplink data signal was transmitted into the 300-m DCF. Since the TFBD, CPS, and TFBC are bidirectional components in the SM core, the uplink data signal can pass through these ones in the reverse direction of the downlink data signal. Finally, after passing through the CPS and CIR in the CO, the transmission performance of the uplink data signal was measured in the uplink receiver in the CO. It should be noted that an EDFA and the following BPF were intentionally located in the uplink receiver, unlike the downlink receiver, because it reduces the power consumption of the RAU needed for optical powering.

III. Improvement of Power Delivery Efficiency

To deliver more electric power to an RAU, it is very important to improve the electric power delivery efficiency of PWoF schemes. Practical ways to achieve this are to reduce the PWoF

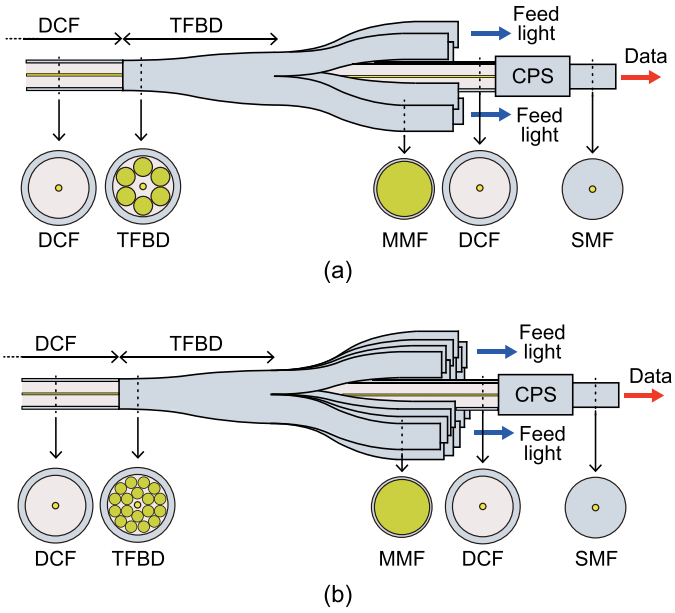

Fig. 3. Configuration of TFBDs with (a) six and (b) 18 MMF output ports.

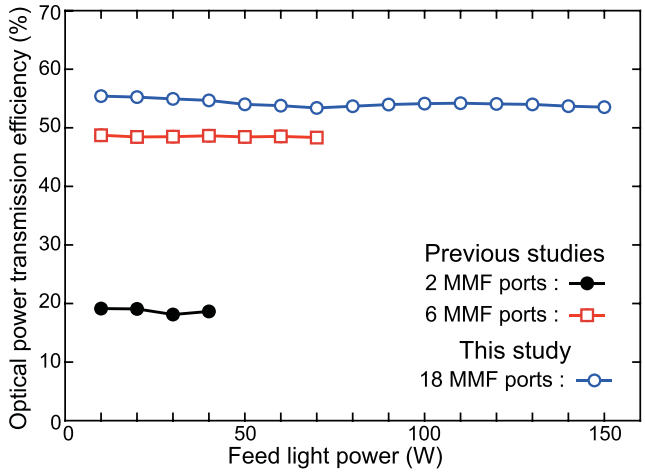

Fig. 4. Optical power transmission efficiency as a function of total feed light power injected into each PWoF link using TFBDs with various numbers of MMF output ports.

link loss, and to improve the O/E conversion efficiency of PPCs. In this article, these two approaches were explored.

A. Tapered Fiber Bundle Divider

As mentioned in Section II, the PWoF link mainly consists of the TFBC, 300-m DCF, and TFBD. Among these components, the TFBC exhibits the smallest transmission loss. In addition, the loss of the DCF is uniquely determined by the fiber length and wavelength of the feed light. Therefore, minimizing the loss in the TFBD as much as possible is a practical approach to improve the electric power delivery efficiency of PWoF schemes.

Fig. 3 shows the configuration of the TFBDs with multiple MMF output ports. In the TFBDs, the feed light power transmitted into the inner cladding of the DCF is extracted by the MMFs. As the feed light propagates through the TFBD, each core of the MMFs gradually thickens, and the feed light is output from each MMF port. In our previous studies, the maximum number of MMF outputs was six [23]−[28], as shown in Fig. 3(a). However, in this article, the feed light that can be extracted by the MMFs from the inner cladding of the DCF was limited, because the feed light component in the non-MMF core area of the inner cladding cannot be extracted by the MMFs. The residual feed light component propagates through the rear DCF and is absorbed in the CPS. Therefore, to increase the feed light power extracted by a TFBD, reducing the non-MMF core area in the TFBD is crucial. In this article, by increasing the number of MMF outputs to 18 ports, as shown in Fig. 3(b), we attempted to reduce the loss in the TFBD, which was a specially customized TFBD we introduced.

Fig. 4 shows the optical power transmission efficiency (OPTE) of the PWoF links using the TFBDs with various numbers of MMF output ports as a function of the total feed light power injected into each PWoF link. Here, the OPTE is defined as the power ratio between the total feed light power injected into each PWoF link and the total feed light power output from all the MMF ports. It can be clearly seen that the OPTEs were almost constant even when the feed light power was changed. In our previous article [25] the average OPTE of the PWoF link using a TFBD with six MMF output ports was approximately 48.5%, whereas in this article, the average OPTE of the PWoF link using a TFBD with 18 MMF output ports was approximately 54.2%. This means that increasing the MMF output ports improved the absolute OPTE by 5.7%. In our theoretical prediction based on the cross-sectional structure of TFBD, the residual feed light loss in the six MMF output ports was 1.8 dB, while the loss in the 18-port MMF output ports was 1.42 dB. Therefore, the loss was predicted to be improved by 0.38 dB. However, the actual loss improvement was 0.24 dB. This was due to the fact that the core of the MMFs was not an ideal round shape because TFBD was made by subsequently fusion splicing the fused, tapered, and cleaved bundle fibers [31]. For comparison, our initial demonstration experiment of the OPTE of the PWoF link using a TFBD with two MMF output ports [22] is also shown by the filled circles in Fig. 4. The average OPTE was approximately 18.5%. These results show that the number of MMF output ports of TFBDs have a significant impact on the OPTE of PWoF links.

B. Photovoltaic Power Converter

There are two important factors that determine the performance of a PPC. One is the O/E conversion efficiency, which is defined as the power ratio between the optical power injected into the PPC and the electric power extracted from the PPC. The other is the maximum optical input power supplied to a PPC. For example, even if the O/E conversion efficiency of a PPC is low, it is possible to extract more electrical power if the maximum optical power that can be input to the PPC is high.

The basic characteristics of two commercially available PPCs are listed in Table I. The O/E conversion efficiency was actually measured in our previous experiment using the HPLD, we used in this article, with a wavelength of 808 nm. Device A was a silicon (Si) based PPC with an O/E conversion efficiency of

TABLE I
BASIC CHARACTERISTICS OF COMMERCIALLY AVAILABLE PPCS

Device (Material)	Maximum input power (W)	Conversion efficiency (%)	Optimum wavelength (nm)
A (Si)	10	24	900–980
B (GaAs)	1.5	55	800–850

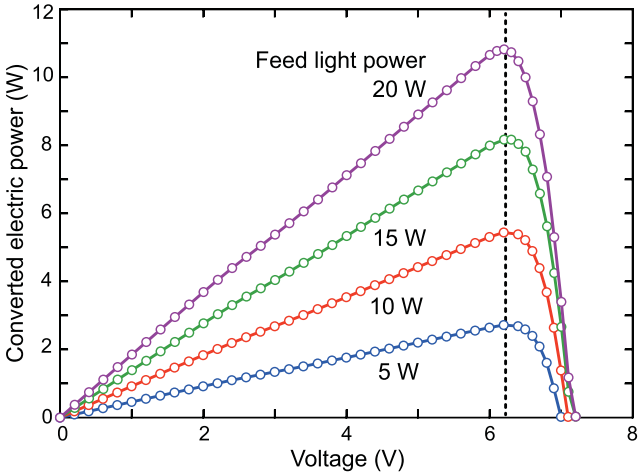

Fig. 5. P–V curves characteristics of PPC for various feed light power injected into PPC at 808 nm. Dashed line shows maximum power point for all feed light power injected into PPC.

24% at 808 nm. It should be noted that the optimal operating wavelength of the PPC was 900−980 nm. The O/E conversion efficiency was approximately 30% in this wavelength range. Although the O/E conversion efficiency was lower than that of device B, the maximum input optical power was much higher. As a result, the Si-based PPC could extract a maximum electric power of 2.4 W when 10 W of feed light power was input to the PPC. Device B was a GaAs-based PPC with an optimum operating wavelength range of 800−850 nm. Although the O/E conversion efficiency was higher than that of the Si-based PPC at 808 nm, the maximum input optical power was lower. As a result, the GaAs-based PPC could extract a maximum electric power of 0.83 W when 1.5 W of feed light power was input to the PPC. Therefore, to increase the electric power extracted by a PPC, it is very important to improve not only the O/E conversion efficiency, but also the maximum input optical power of the PPC.

In this article, to improve the electric power delivered to the RAU, we used a customized GaAs-based PPC based on the vertical epitaxial monolithic heterostructure architecture design [29], [30]. The device provides higher capability both of O/E conversion efficiency and available input optical power than those of conventional PPCs. To demonstrate its performance, we measured the power–voltage (P–V) curve characteristics of the PPC for various feed light powers injected into the PPC, as shown in Fig. 5. As a feed light source for this measurement, we used one of the HPLDs at a wavelength of 808 nm, as shown in Fig. 2. As the voltage for an electric load was increased, the converted electric power was linearly increased. The maximum electric power was obtained at approximately 6.2 V, and the voltage was called the maximum power point (MPP), as shown

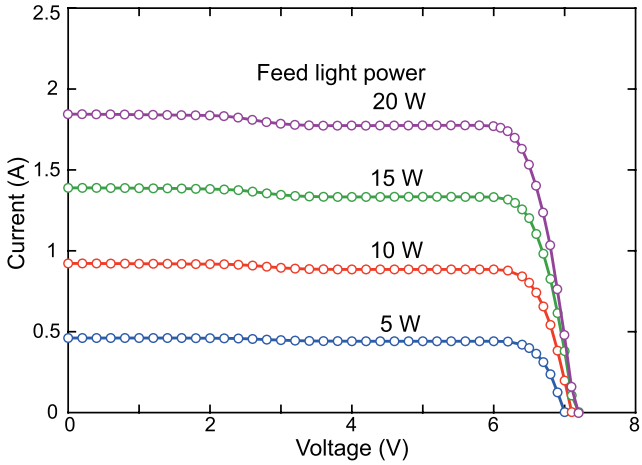

Fig. 6. I–V curves characteristics of PPC for various feed light power injected into PPC at 808 nm.

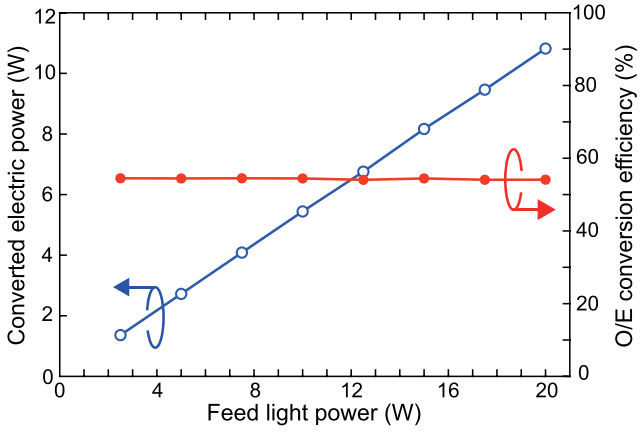

Fig. 7. Converted electric power and O/E conversion efficiency of PPC as a function of feed light power injected into PPC.

in the dashed line in Fig. 5. After that, the power was decreased as the voltage was increased. The same characteristics were observed even when the feed light power was changed, and the same MPP was obtained for all the feed light powers.

Fig. 6 shows the current–voltage (I–V) curve characteristics of the PPC as a function of the feed light power injected into the PPC. The current was almost constant even when the voltage for an electric load was increased. However, the current suddenly decreased after the MPP. The same trend was observed even when the feed light power was changed and for the P–V curve characteristics.

To determine the performance of the PPC, we measured the converted electric power and the O/E conversion efficiency as a function of the feed light power injected into the PPC at the MPP, as shown in Fig. 7. As the feed light power increased, the converted electric power was linearly increased. For the 20-W feed light injection, an electric power of over 10 W was obtained. The O/E conversion efficiency was almost constant regardless of the feed light power, and the average O/E conversion efficiency was approximately 54%, as shown in Fig. 7. The results show

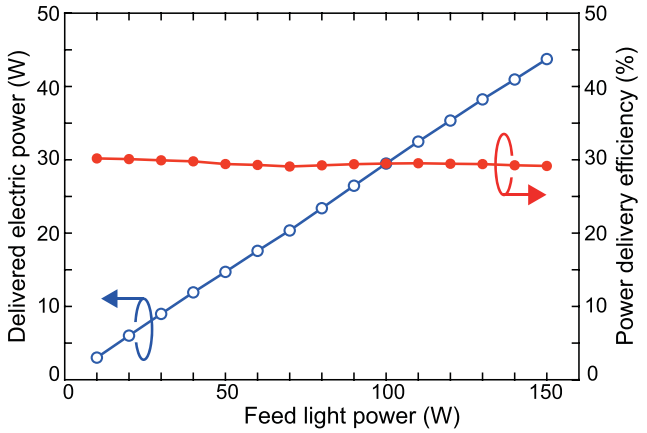

Fig. 8. Delivered electric power and power delivery efficiency of PWoF scheme as a function of total feed light power injected into PWoF scheme.

that the use of the PPC is effective in improving the delivered electric power of the PWoF scheme.

IV. Simultaneous Electric Power Delivery and Optical Data Transmission

To evaluate the power transmission performance of the PWoF scheme, we measured the delivered electric power and power delivery efficiency of the PWoF scheme, as shown in Fig. 8. Here, the power delivery efficiency is defined as the power ratio between the total feed light power injected into the PWoF link and the total electric power converted by the PPC. As the total feed light power increased, the delivered electric power was linearly increased up to 43.7 W. The linear characteristics are very useful for controlling the electric power supplied to the RAUs. As mentioned in Section I, the power control by PWoF is an attractive function for changing the power supplied to RAUs in response to the temporary mobile data traffic of each RAU, and it is expected that the power consumption of the entire network will be efficiently reduced. The power delivery efficiency was almost constant regardless of the feed light power, and the average efficiency was approximately 30%. As shown in Section III, the improved TFBD design and the high-performance PPC greatly contributed to an increase in the delivered electric power of the PWoF link.

In simultaneous power and data signal transmission by PWoF using a single optical fiber, it is very important not only to deliver higher power electric power but also to transmit data signals with a good transmission performance. To evaluate the transmission performance of the simultaneously downlink- and uplink-transmitted data signals, we measured the EVM characteristics of the electrical back-to-back and transmitted signals, as shown in Fig. 9. EVM is a well-known measure of signal quality for digital communication systems. The smaller the value, the better the signal quality. Back-to-back signals are transmitted directly between a transmitter and a receiver and do not pass along a transmission line. In this setup, it means that the data signals generated by the downlink and uplink transmitters are directly received at the downlink and uplink receivers, respectively. Fig. 9 shows the EVM curves of the

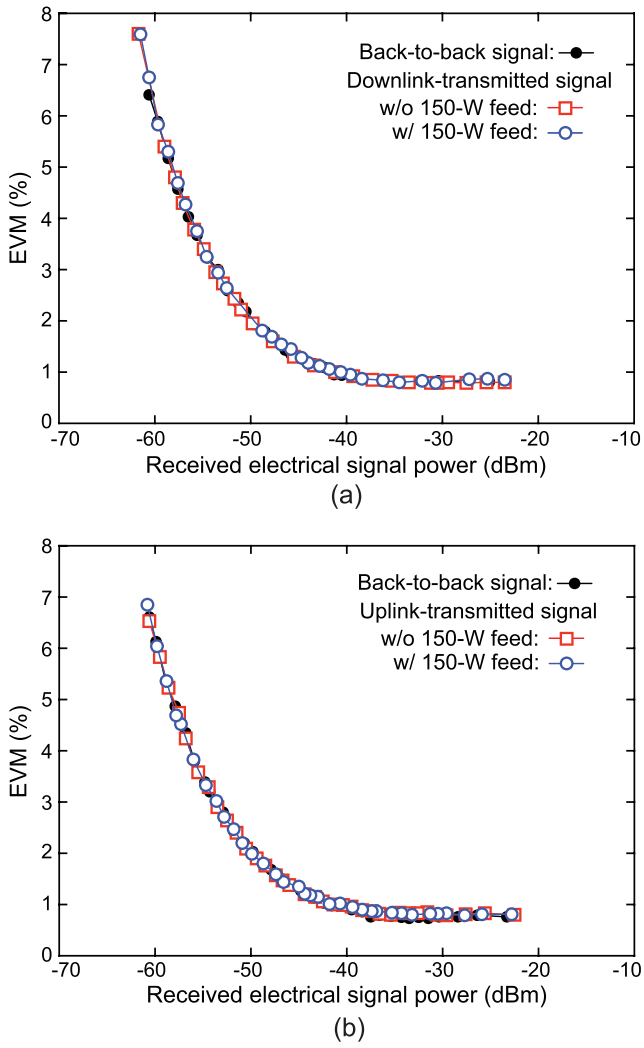

Fig. 9. EVM curves of (a) back-to-back and downlink-transmitted signals and (b) back-to-back and uplink-transmitted data signals with (w/) and without (w/o) 150-W PWoF feed as a function of received electrical signal power.

back-to-back and transmitted signals, with (w/) and without (w/o) 150-W PWoF feed, as a function of the received electrical signal power. As the received power was increased, the EVM preserved high signal quality. When the received power was larger than −38 dBm, the EVM values became almost constant at approximately 0.9%. Furthermore, the 150-W PWoF feed showed no significant difference in the EVM characteristics. It should be noted that the transmitter and receiver blocks in the CO and RAU are slightly different, as mentioned in Section II. However, the performance difference between the downlink and uplink transmission in terms of EVM measurement was not observed.

Fig. 10 shows variations in the EVM penalties to the back-to-back signal of the simultaneously downlink- and uplink-transmitted data signals with the total feed light power injected into the PWoF link. In the both cases, the EVM values were almost constant, and the variations were less than 0.05% even when the feed light power was increased up to 150 W. The insets show the constellations of these signals when the feed light

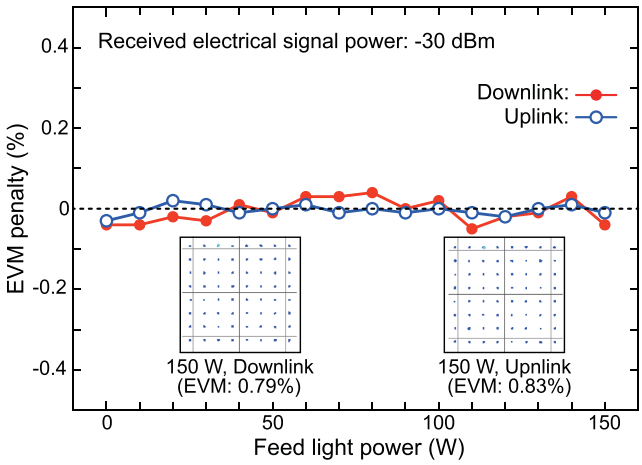

Fig. 10. EVM penalties to back-to-back signal of downlink- and uplink-transmitted data signals as a function of total feed light power injected into PWoF link. Insets show constellations of downlink- and uplink-transmitted data signals with 150-W PWoF feed.

power was set to 150 W. The EVM values of the downlink- and uplink-transmitted signals were 0.79% and 0.83%, respectively. The result shows that these signals have good transmission performances even when electric power greater than 40 W is simultaneously delivered into the same optical fiber.

V. Discussion

In this article, the transmission loss of the PWoF scheme was reduced by the improved TFBD design, and a high-performance PPC was introduced to improve the delivered electric power. On the other hand, for HPLDs, we used commercially available conventional LDs. The electrical-to-optical (E/O) conversion efficiency of the HPLDs was approximately 40%. Therefore, the electric-to-electric power transmission efficiency in the entire PWoF scheme was approximately 12%. We selected the HPLDs based only on the specifications of the output wavelength and the maximum output power. However, it is expected that the transmission efficiency of electric power can be further improved by using HPLDs with a higher E/O conversion efficiency.

To reduce the transmission loss of the PWoF link, the number of output ports of the TFBD was increased from 6 to 18. In principle, the number of ports can be further increased to reduce the feed light power that leaks out into the CPS at the output of the TFBD. However, as the TFBD with 18 MMF output ports was a specially customized component, it was very difficult to further increase the number of MMF output ports. In addition, as the number of MMF output ports increases, the number of PPCs required increases. For these reasons, we think that the 18 MMF output ports are optimal for minimizing the insertion losses of the feed light in TFBDs.

VI. Conclusion

We successfully demonstrated the simultaneous transmission of up to 43.7 W of electric power and bidirectional data signals using a 300-m DCF. To increase the power transmission efficiency of a PWoF link, we improved the design of the PWoF link in order to transmit higher feed light power into the PWoF link. Furthermore, to increase the delivered electric power, we introduced a specially customized PPC. To the best of the authors' knowledge, this is the highest electric power delivery demonstration by PWoF with data signals using a single optical fiber. Even when the PWoF feed was increased up to 150 W, the data signals exhibited good transmission performances. The results show that the PWoF using a DCF can simultaneously deliver data signals and electric power for driving a small to mid-sized RAU for RoF-based mobile communication networks.

References

[1] R. C. Miller and R. B. Lawry, "Optically powered speech communication over a fiber lightguide," *Bell Syst. Tech. J.*, vol. 58, no. 7, pp. 1735–1741, Sep. 1979.
[2] T. C. Banwell, R. C. Estes, L. A. Reith, P. W. Shumate, and E. M. Vogel, "Powering the fiber loop optically—A cost analysis," *IEEE J. Lightw. Technol.*, vol. 11, no. 3, pp. 481–494, Mar. 1993.
[3] R. Penã, C. Algora, I. R. Matías, and M. López-Amo, "Fiber-based 205-mW (27% efficiency) power-delivery system for an all-fiber network with optoelectronic sensor units," *Appl. Opt.*, vol. 38, no. 12, pp. 2463–2466, Apr. 1999.
[4] H. Miyakawa, Y. Tanaka, and T. Kurokawa, "Design approaches to power-over-optical local-area-network systems," *Appl. Opt.*, vol. 43, no. 6, pp. 1379–1389, Feb. 2004.
[5] J.-G. Werthen, "Powering next generation networks by laser light over fiber," in *Proc. Conf. Opt. Fiber Commun./Nat. Fiber Opt. Eng. Conf.*, OWO3, Mar. 2008, Paper OWO3.
[6] G. Böttger *et al.*, "An optically powered viode camera link," *IEEE Photon. Technol. Lett.*, vol. 20, no. 1, pp. 39–41, Jan. 2008.
[7] X. Zhang *et al.*, "A gate drive with power over fiber-based isolated power supply and comprehensive protection functions for 15-kV SiC MOSFET," *IEEE J. Emerg. Sel. Top. Power Electron.*, vol. 4, no. 3, pp. 946–955, Sep. 2016.
[8] M. Sauer, A. Kobyakov, and J. George, "Radio-over-fiber for pico-celler network architectures," *IEEE J. Lightw. Technol.*, vol. 25, no. 11, pp. 3301–3320, Nov. 2007.
[9] I. A. Alimi, A. L. Teixeira, and P. P. Monteiro, "Toward an efficient C-RAN optical fronthaul for the future networks: A tutorial on technologies, requirements, challenges, and solutions," *IEEE Commun. Surveys Tut.*, vol. 20, no. 1, pp. 708–769, Jan.–Mar. 2018.
[10] P. Frenger, C. Friberg, Y. Jading, M. Olsson, and O. Persson, "Radio network energy performance: Shifting focus from power to precision," *Ericsson Rev.*, vol. 91, no. 2. pp. 1–9, Feb. 2014.
[11] I. Ashraf, F. Boccardi, and L. Ho, "SLEEP mode techniques for small cell deployments," *IEEE Commun. Mag.*, vol. 49, no. 8, pp. 72–79, Aug. 2011.
[12] K. Sone, I. Kim, X. Wang, Y. Aoki, H. Seki, and J. C. Rasmussen, "Analysis of power consumption in mobile backhaul network with densely deployed small cells under dynamic traffic behavior," in *Proc. Optoelectron. Commun. Conf./Int. Conf. Photon. Switching.*, TuA4-2, Niigata, Japan, Jul. 2016, Paper TuA4-2.
[13] H. Kuboki and M. Matsuura, "Optically powered radio-over-fiber system based on center- and offset-launching techniques using a conventional multimode fiber," *Opt. Lett.*, vol. 43, no. 5, pp. 1057–1070, Mar. 2018.
[14] D. Wake, A. Nkansah, N. J. Gomes, C. Lethien, C. Sion, and J.-P. Vilcot, "Optically powered remote units for radio-over-fiber systems," *J. Lightw. Technol.*, vol. 26, no. 15, pp. 2484–2491, Aug. 2008.
[15] C. Lethien *et al.*, "Energy-autonomous picosecond remote antenna unit for radio-over-fiber system using the multiservice concept," *Photon. Technol. Lett.*, vol. 24, no. 8, pp. 649–651, Apr. 2012.
[16] M. Kama, M. Toyonaga, N. Ogawa, H. Tanase, M. Awamori, and K. Anzai, "Development of new aerial optical cable and closure that allow subsequent closure installation," *NTT Techn. Rev.*, vol. 5, no. 8, pp. 1–5, Aug. 2007.
[17] H. Helmers, C. Armbruster, M. Ravenstein, D. Derix, and C. Schöner, "6 W optical power link with integrated optical data transmission," *IEEE Trans. Power Electron.*, vol. 35, no. 8, pp. 7904–7909, Aug. 2020.
[18] M. R. Singh, "A study of optoelectronics in photonic nanowires made from photonic crystals," *Appl. Phys. B*, vol. 93, no. 1, pp. 91–98, Oct. 2008.
[19] M. R. Singh, "Photon transparency in metallic photonic crystals doped with an ensemble of nanoparticles," *Phys. Rev. A*, vol. 79, no. 1, Jan. 2009, Art. no. 013826.

[20] J. D. Cox, M. R. Singh, C. Racknor, and R. Agrawal, "Switching in polaritonic—photonic crystal nanofibers doped with qunatum dots," *Nano Lett.*, vol. 11, no. 12, pp. 5284–5289, Oct. 2011.
[21] M. Matsuura and J. Sato, "Bidirectional radio-over-fiber systems using double-clad fibers for optically powered remote antenna units," *IEEE Photon. J.*, vol. 7, no. 1, Feb. 2015, Art. no. 7900609.
[22] J. Sato, H. Furugori, and M. Matsuura, "40-Watt power-over-fiber using a double-clad fiber for optically powered radio-over-fiber systems," in *Proc. Opt. Fiber Commun. Conf. Exhib.*, Mar. 2015, Paper W3F.6.
[23] M. Matsuura, H. Furugori, and J. Sato, "60 W power-over-fiber feed using double-clad-fibers for radio-over-fiber systems with optically powered remote antenna units," *OSA Opt. Lett.*, vol. 40, no. 23, pp. 5598–5601, Dec. 2015.
[24] M. Matsuura and Y. Minamoto, "Optically powered and controlled beam steering system for radio-over-fiber networks," *IEEE J. Lightw. Technol.*, vol. 35, no. 4, pp. 979–988, Feb. 2017.
[25] D. Kamiyama, A. Yoneyama, and M. Matsuura, "Multichannel data signals and power transmission by power-over-fiber using a double-clad fiber," *IEEE Photon. Technol. Lett.*, vol. 30, no. 7, pp. 646–649, Apr. 2018.
[26] M. Matsuura, "Optically powered radio-over-fiber systems," in *Proc. Conf. Lasers Electro-Opt.*, May 2018, Paper SM1C.3.
[27] M. Matsuura, "Over 100-W power-over-fiber for remote antenna units," in *Proc. 1st Opt. Wireless Fiber Power Transmiss. Conf.*, Yokohama, Japan, Apr. 2019, Paper OWPT-5-01.
[28] M. Matsuura, N. Tajima, H. Nomoto, and D. Kamiyama, "150-W power-over-fiber using double-clad fibers," *IEEE J. Lightw. Technol.*, vol. 38, no. 2, pp. 401–408, Jan. 2020, PaperOWPT-5-01.
[29] S. Fafard *et al.*, "Ultrahigh efficiencies in vertical epitaxial heterostructure architectures," *Appl Phys. Lett.*, vol. 108, no. 7, Feb. 2016, Art. no. 071101.
[30] S. Fafard *et al.*, "High-photovoltage GaAs vertical epitaxial monolithic heterostructures with 20 thin p/n junctions and a conversion efficiency of 60%," *Appl Phys. Lett.*, vol. 109, no. 13, Sep. 2016, Art. no. 131107.
[31] A. Kosterin, V. Temyanko, M. Fallahi, and M. Mansuripur, "Tapered fiber bundles for combining high-power diode lasers," *Appl. Opt.*, vol. 43, no. 19, pp. 3893–3900, Jul. 2004.

Motoharu Matsuura (Senior Member, IEEE) received the Ph.D. degree in electrical engineering from the University of Electro-Communications, Tokyo, Japan, in 2004.

In 2007, he joined as an Assistant Professor with the Department of Information and Communication Engineering, University of Electro-Communications, where he is currently a Professor of the Graduate School of Informatics and Engineering. From 2010 to 2011, on leave from the university, he joined as a Visiting Researcher with the COBRA Research Institute with the Eindhoven University of Technology, Eindhoven, The Netherlands, where he studied ultrahigh-speed optical signal processing using semiconductor-based devices. His research interests include optical signal processing, photonic subsystems, and radio-over-fiber transmission systems. He is the author or coauthor of more than 220 papers published in international refereed journals and conferences, including OFC and ECOC Postdeadline Papers and OFC Top Scored Papers.

Dr. Matsuura was the recipient of the Ericsson Young Scientist Award in 2008, the FUNAI Information Technology Award for Young Researcher in 2009, and Telecommunication System Technology Award of the Telecommunications Advancement Foundation (TAF) in 2011. He is a member of the Optical Society of America and the Institute of Electronics, Information, and Communication Engineers.

Hayato Nomoto received the B.E. degree in 2018 from the University of Electro-Communications, Tokyo, Japan, where he is currently working toward the master's degree with the Department of Communication and Network Engineering.

His research interests include radio-over-fiber (RoF) transmission systems and the subsystems.

Hikaru Mamiya received the B.E. degree in 2019 from the University of Electro-Communications, Tokyo, Japan, where he is currently working toward the master's degree with the Department of Communication and Network Engineering.

His research interests include radio-over-fiber (RoF) transmission systems and the subsystems.

Tadanobu Higuchi received the B.E. degree from Nihon University, Chiba, Japan, in 2018. He is currently working toward the master's degree with the Department of Communication and Network Engineering, University of Electro-Communications, Tokyo, Japan.

His research interests include radio-over-fiber (RoF) transmission systems and the subsystems.

Denis Masson was born in Rimouski, Canada. He received the degree in physics and M.Sc. degrees from the University of Ottawa, Ottawa, ON, Canada, and the Ecole Polytechnique de Montreal, Montreal, QC, Canada, and the Ph.D. degree in applied and engineering physics from Cornell University, Ithaca, NY, USA, in 1991.

He specializes in the design and fabrication of optically active III-V compound semiconductor devices and has worked for Nortel and ST Micro-Electronics as well as startup companies such as MetroPhotonics, Cyrium Technologies, ArtIC Photonics, and Azastra Opto, where he was the Co-Founder. He currently works for Broadcom, IFPD division, Ottawa, ON, Canada.

Simon Fafard received the Ph.D. degree in physics from the University of Ottawa, Ottawa, ON, Canada, in 1992.

He was an NSERC Postdoctoral Fellow with the Center for Quantized Electronic Structures, University of California, Santa Barbara (UCSB), Santa Barbara, CA, USA. He is currently a Hardware Specialist with Broadcom, IFPD division, Ottawa, ON, Canada, which is a large public corporation that acquired Azastra, where he was a Co-Founder and President. He focuses on the design, epitaxy, and characterization of optoelectronic devices. He has more than 25 years of experience in optoelectronics and photonics while developing and commercializing numerous devices and products in the industry. He also worked as a Professor with Université de Sherbrooke, Sherbrooke, QC, Canada, as a Senior Research Officer with National Research Council, and as an Adjunct Professor in Physics with the University of Ottawa. He has authored more than 300 publications that received more than 12 000 citations. He is the inventor of more than 30 patents. He raised over $20 M of private and venture capital funding and also obtained numerous research grants.

Dr. Fafard was the recipient of the 2017 CAP Medal for Outstanding Achievement in Industrial and Applied Physics.